Am J Cancer Res 2024;14(8):3694-3710
www.ajcr.us /ISSN:2156-6976/ajcr0155873

Original Article

Paraneoplastic leukocytosis induces NETosis and thrombosis in bladder cancer PDX model

Yung-Chia Kuo[1], Chen-Yang Huang[1], Cedric Chuan Young Ng[2], Chiao-Yun Lin[3], Wen-Kuan Huang[1], Li-Yu Lee[4], Hsien-Chi Fan[1], An-Chi Lin[1], Kai-Jie Yu[5], See-Tong Pang[5], Bin Tean Teh[6,7], Cheng-Lung Hsu[1]

*[1]Division of Hematology-Oncology, Department of Internal Medicine, Chang Gung Memorial Hospital at Linkou, Chang Gung University, Taoyuan 33305, Taiwan; [2]Integrated Genomics Platform, National Cancer Centre Singapore, Singapore, The Republic of Singapore; [3]Gynecologic Cancer Research Center, Chang Gung Memorial Hospital at Linkou, Chang Gung University, Taoyuan 33305, Taiwan; [4]Department of Pathology, Chang Gung Memorial Hospital at Linkou, Chang Gung University, Taoyuan 33305, Taiwan; [5]Division of Urology, Department of Surgery, Chang Gung Memorial Hospital at Linkou, Chang Gung University, Taoyuan 33305, Taiwan; [6]Institute of Molecular and Cell Biology, Agency for Science, Technology and Research (A*STAR), Singapore, The Republic of Singapore; [7]Duke-NUS Medical School, Singapore, The Republic of Singapore*

Received February 11, 2024; Accepted May 8, 2024; Epub August 25, 2024; Published August 30, 2024

Abstract: Paraneoplastic leukocytosis (PNL) in genitourinary cancer, though rare, can indicate aggressive behavior and poor outcomes. It has been potentially linked to cancer expressing G-CSF and GM-CSF, along with their respective receptors, exerting an autocrine/paracrine effect. In our study, we successfully established four patient-derived xenograft (PDX) lines and related cell lines from urothelial cancer (UC), conducting next-generation sequencing (NGS) for genetic studies. UC-PDX-LN1, originating from bladder cancer, exhibited two druggable targets - *HRAS* and *ERCC2* - responding well to chemotherapy and targeted therapy, though not to tipifarnib, an *HRAS* inhibitor. Transcriptome analysis post-treatment illuminated potential mechanisms, with index protein analysis confirming their anticancer pathways. Mice implanted with UC-PDX-LN1 mirrored PNL observed in the patient's original tumor. Cytokine array and RT-PCR analyses revealed high levels of G-CSF and GM-CSF in our PDX and cell lines, along with their presence in culture media and tumor cysts.Leukocytosis within small vessels in and around the tumor, associated with NETosis and thrombus formation, suggested a mechanism wherein secreted growth factors were retained, further fueling tumor growth via autocrine/paracrine signaling. Disrupting this cancer cell-NETosis-thrombosis cycle, we demonstrated that anti-neutrophil or anticoagulant interventions enhanced chemotherapy's antitumor effects or prolonged survival in mice, even though these drugs lacked direct antitumor efficacy when used independently. Clinical observations in bladder cancer patients revealed PNL in 1.61% of cases (35/2162) with associated poor prognosis. These findings propose a novel approach, advocating for the combination of anticancer/NETosis/thrombosis strategies for managing UC patients presenting with PNL in clinical settings.

Keywords: Paraneoplastic leukocytosis, patient-derived xenograft, NETosis, autocrine, thrombosis, bladder cancer

Introduction

Tumors can secrete hematopoietic growth factors like G-CSF and GM-CSF while expressing their respective receptors, initiating an autocrine/paracrine loop that stimulates rapid tumor growth [1-3]. These tumor-secreted factors are pivotal in reprogramming the bone marrow, leading to a bias towards myelopoiesis expansion. This results in the production and mobilization of mature and immature granulocytic populations in the peripheral blood and their accumulation in the tumor microenvironment (TME) [4, 5]. Within the context of cancer, tumor-associated neutrophils (TANs) exhibit a heterogeneous nature, playing a dual role in the tumor microenvironment. While some TANs contribute to tumor-promoting inflammation by driving processes such as angiogenesis, extracellular remodeling, metastasis, and immunosuppression, others mediate direct tumor killing and cooperate in antitumor cellular networks [6]. While paraneoplastic leukocytosis (PNL) is relatively uncommon in bladder cancer

https://doi.org/10.62347/IHIO5742

(BC), it can be observed in up to 10% of solid tumors [7]. This association is linked to aggressive clinical behavior, systemic inflammatory response syndrome, and poor outcomes [8, 9]. Notably, leukocyte count and serum G-CSF levels in PNL may return to normal after the surgical removal of bladder tumors, correlating with long-term survival. These parameters can serve as indices for monitoring treatment response [10].

Neutrophils serve as the frontline defense against microbial infections, employing mechanisms such as phagocytosis, degranulation, and NETosis - a process where neutrophils release extracellular fibers (NETs) composed of modified chromatin adorned with bactericidal cytosolic granules and proteins [11]. While initially identified as an immune response to bacterial infections, NETosis is now recognized to occur abnormally in various inflammatory processes, including cancer [12]. In tumor-bearing animal models, NETosis can awaken dormant cancer cells by releasing proteases like neutrophil elastase and matrix metalloproteinase 9. These proteases activate the laminin-integrin pathway and degrade thrombospondin-1 (TSP-1), inducing cancer cell proliferation [13, 14]. Tumors may secrete chemotactic ligands for CXCR1/2, recruiting neutrophils to form NETs that create a physical shield around cancer cells, protecting them from immune cell attacks. NETosis inhibition could sensitize tumors to immune checkpoint inhibitor treatments [15]. NETs promote circulating tumor cell metastasis by sequestering tumor cells [16], enhancing migration and invasion [17], and augmenting treatment, with the NET-digesting enzyme, DNase I, markedly reducing metastasis [18]. Cancer-related NETosis is also implicated in inducing systemic thromboembolism, associated with elevated proinflammatory cytokines and adhesion molecules, compromising the function of distant organs [19].

We successfully established four patient-derived xenograft (PDX) lines from clinical GU patients presenting with PNL. Utilizing next-generation sequencing (NGS) studies, we identified potential druggable targets, including the presence of an *ERCC2* mutation. Drug screening using the PDX model confirmed the effectiveness of certain anticancer medications. Additionally, the PDX-implanted mice exhibited PNL, mirroring the condition observed in the patient from whom the PDX was derived. The detailed characterization of this PDX line contributes valuable information for clinical management, offering insights into potential therapeutic targets and providing a preclinical platform for testing anticancer drugs specific to the patient's condition.

Materials and methods

Drugs

Palbociclib (Ibrance) was purchased from Pfizer Manufacturing Deutschland GmbH (Freiburg, Germany). Sunitinib was bought from Pfizer Italia S.R.L. (Ascoli Piceno, Italy). Ladarixin was available from Dompé Farmaceutici SpA (L'Aquila AQ, Italy). Rivaroxaban was purchased from Bayer AG (Leverkusen, Germany).

Patients

Blood and tumor samples from patients with UC for PDX establishment were prospectively collected after obtaining written informed consent between January 2017 and July 2021 at CGMH. This study was approved by the Institutional Review Board of CGMH (IRB No. 201801741A3).

UC PDX establishment

PDX models were generated as described in our previous study [20].

Whole-exome sequencing

DNA for whole-exome sequencing (WES) was extracted from PDX and PDX-derived cell lines. The detailed method has been previously described [21].

Cell growth assay and animal studies

UC cell lines, U5637 (from ATCC) and UC-LN1 cell line (derived from UC-PDX-LN1 with more than 60 passages *in vitro*) were maintained in RPMI containing 10% fetal bovine serum (FBS). A cell growth assay and animal studies were conducted as described previously [20, 22]. All experiments involving laboratory animals followed the guidelines for animal experiments of Chang Gung Memorial Hospital (CGMH) and were approved by the IACUC of CGMH (IACUC no. 2018092107).

Bulk RNA sequencing and differential expression analysis

The detailed method has been previously described [22].

Plasma cytokine array analysis

The ARY022 cytokine array assay kit (R&D Systems, Minneapolis, MN, USA) was performed according to the manufacturer's instructions, as previously described [22].

Antibodies

One hundred micrograms of the protein lysate per lane were used for Western blot analysis. Antibodies used in this study were as follows: G-CSF (Abcam ab197993), G-CSFR (Abcam ab126167), GM-CSF (Santa Cruz Biotechnology SC-32753), GM-CSFR (Santa Cruz Biotechnology SC-21764, SC-456), Histone 3 (citrulline R2 + R8 + R17, Abcam ab5103), Ly6G (eBioscience 17-9668-82), Cleaved PARP (Cell Signaling Technology 95465), p-FGFR1/2/3/4 (Proteintech 11935-1-AP), FGFR2 (Signalway Antibody 32586), p-STAT3 (Cell Signaling Technology 9145), STAT3 (Cell Signaling Technology 12640), γ-H2AX (Santa Cruz Biotechnology SC-517348), MMP1 (Gene Tex GTX100534), and β-actin (Santa Cruz Biotechnology SC-47778).

Statistical analysis

Tumor weight data are presented as mean ± SD. The final tumor volume was compared using a two-tailed analysis of variance (ANOVA). Overall survival, which was calculated from the time of recurrence or metastasis to death, was examined by plotting Kaplan-Meier curves and compared using the log-rank test. In all analyses, *p*-values were two-tailed, and data were considered statistically significant at a p-value < 0.05.

Results

We have recently successfully established four patient-derived xenograft (PDX) lines and two PDX-derived cell lines, UC-LN1 and UC-B1, originating from UC-PDX-LN1 and UC-PDX-B1, respectively. Both are derived from bladder urothelial cell carcinoma within the context of genitourinary (GU) cancers, as illustrated in **Table 1**. Utilizing next-generation sequencing (NGS) studies, we identified two druggable targets, *HRAS* and *ERCC2* (excision repair cross-complementation group 2), in both UC-PDX-LN1 and UC-LN1. However, no druggable targets were identified in PDX-B1 and UC-B1. The *HRAS* mutation, Gln61Lys, suggests potential responsiveness to Tipifarnib [23], while the *ERCC2* mutation, Asn238Ser, may exhibit sensitivity to cisplatin treatment [24] as demonstrated in **Figure 1A**. Subsequent confirmation of these mutations through target sequencing is presented in **Figure 1B** and **1C**. Importantly, UC-PDX-LN1 faithfully represents the cellular characteristics of its parent tumor from the patient, as demonstrated in **Figure 1D**.

The original patient with UC-PDX-LN1 exhibited intratumor cystic changes and leukocytosis with a neutrophil-dominant profile, indicative of paraneoplastic leukocytosis in a clinical setting. In mice implanted with UC-PDX-LN1, we observed intratumor cystic changes via PET scan (**Figure 2A**) and leukocytosis dominated by neutrophils and splenomegaly (**Figure 2B**, **2D** and **2E**). Additionally, the mice exhibited symptoms such as body weight loss, decreased appetite and activity, cachexia, and even sudden death, despite the implanted tumor not reaching 2000 mm^3. We conducted a pilot drug test for UC-PDX-LN1 to explore potential therapeutic options. All tested candidate drugs, except tipifarnib, demonstrated inhibitory effects on xenograft growth with statistical significance compared to the control, as illustrated in **Figure 2**. The IC50 of cisplatin, gemcitabine, sunitinib, and tipifarnib were measured in UC-LN1, UC-B1, and UC5637 cell lines (see Supplementary Figure 1). Leukocytosis observed in mice implanted with UC-PDX-LN1 was alleviated through effective anticancer treatment. This improvement correlated with drug response, as depicted in **Figure 2E**. The antitumor efficacy of chemotherapy with gemcitabine combined with cisplatin (G+P), targeted therapy with sunitinib, or their combination resulted in significant inhibition of UC-PDX-LN1 growth, leading to prolonged survival, as illustrated in **Figure 2F** and **2G**. To further investigate the drug response, we tested G+P, sunitinib, and combination treatments in another PDX line, UC-PDX-B1, which exhibited gemcitabine resistance and no leukocytosis in the PDX-implanted mice. The drug test revealed

Table 1. Characteristics of total 4 UC patients with PDX and cell lines

Patient No.	Age (y/o)	Gender	Dignosis		Status at biopsy/operation		Previous treatment	PDX	Cell line	Overall survival from PDX (months)	alive/ expired
			primary site	cell type	Tissue sourece	Biopsy(B)/ Excision(E)					
1	89	female	renal pelvis	urothelial carcinoma (UC)	renal pelvis	E	no	UGUC-PDX1	UGUC-1	4	expired
2	60	male	bladder	papillary UC	bladder	E	operation	UC-PDX1	UC-1	100	alive
3	67	male	bladder	UC	bone	B	chemotherapy, radiotherapy	UC-PDX-B1	UC-B1	7	expired
4	53	female	bladder	UC	lymph node	B	chemotherapy, operation	UC-PDX-LN1	UC-LN1	3	expired

A

UC-PDX-LN1 druggable mutation

Sample	Gene	Variant Type	HGVS	LEVEL 3B
UC-PDX-LN1	HRAS	Missense Mutation	c.181C>A	Tipifarnib
UC-PDX-LN1	ERCC2	Missense Mutation	c.713A>G	Cisplatin
UC-LN1	HRAS	Missense Mutation	c.181C>A	Tipifarnib
UC-LN1	ERCC2	Missense Mutation	c.713A>G	Cisplatin

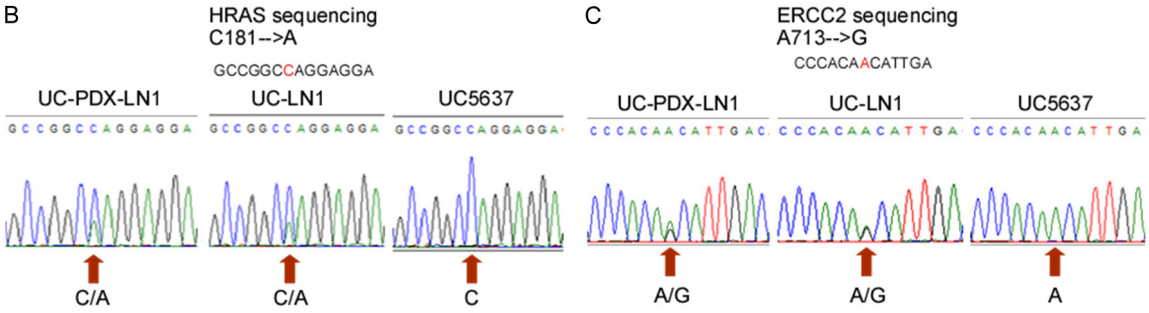

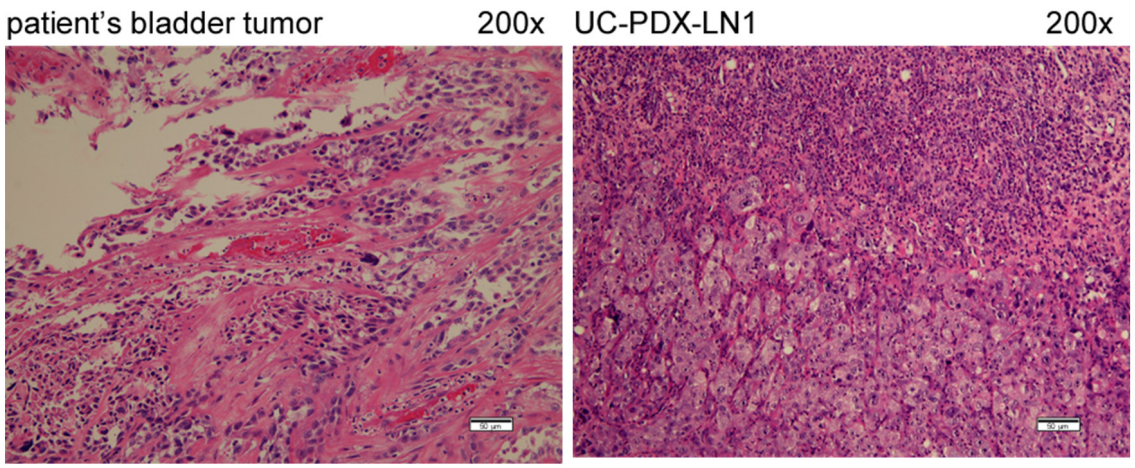

Figure 1. Characterization of a newly established UC-PDX-LN1. (A) NGS, SNP showed two druggable mutations in *HRAS* and *ERCC2*. Targeting sequencing confirmed these *HRAS* (B) and *ERCC2* (C) mutations. (D) H&E staining of the patient's bladder tumor and PDX.

G+P resistance but sensitivity to sunitinib, with no additional synergistic effect in combination treatment, as exhibited in **Figure 2H-J**.

Treatment with sunitinib, a multi-kinase inhibitor, in the UC-PDX model influenced multiple metabolic processes and muscle structure development, as illustrated in **Figure 3A**. Conversely, treatment with gemcitabine plus cisplatin (G+P) in the UC-PDX model induced significant upregulation and downregulation of genes associated with the suppression of metabolic processes and cell division, as exhibited in **Figure 3B**. In the case of the sunitinib-G+P combination treatment in the UC-PDX model, there was an association between the suppression of cell migration and the activation of muscle fiber development, compared to the effects of each agent alone, as illustrated in **Figure 3C**. These findings likely reflect the distinct drug characteristics within the biological context.

Urothelial carcinoma (UC) treated with gemcitabine plus cisplatin (G+P), a cytotoxic chemotherapy known for posing a constant threat to DNA integrity and cellular processes, displayed dysfunctions in γ-H2AX, a crucial factor in the double-strand breaks response, ultimately driving towards genomic instability [25]. This observation aligns with signature-enriched

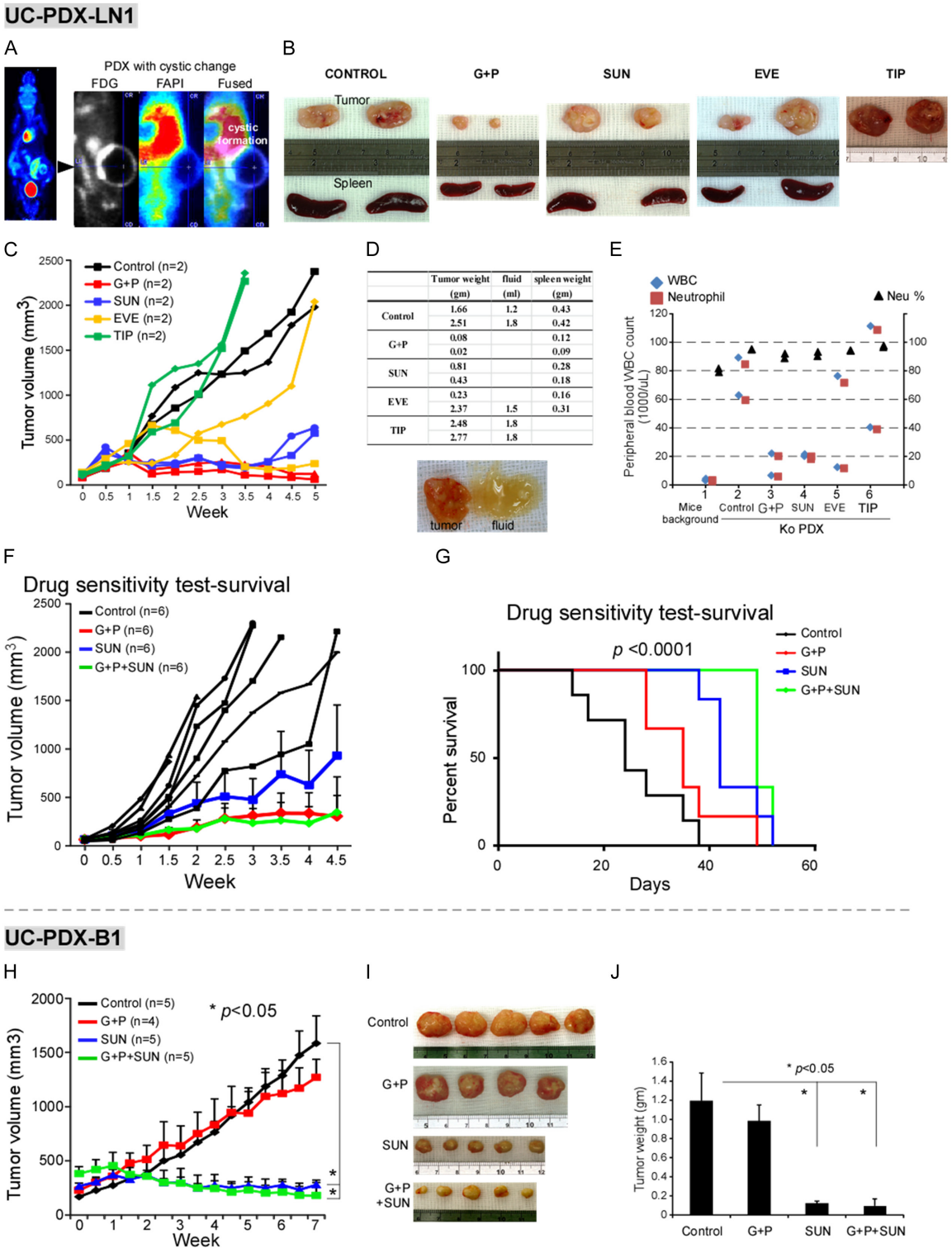

Figure 2. Drug sensitivity test in UC-PDX. (A-G) UC-PDX-LN1, (A) PDX with cystic change in FDG-PET image. (B) Gross tumor and spleen, (C) Tumor volume change, (D) Tumor weight in different treatments. Some large tumors had cystic change with fluid accumulation. (E) Change in peripheral blood white blood cell count in response to different treatments in (B). (F, G) UC-PDX-LN1 mice survival in response to different treatments. Another UC-PDX line, UC-PDX-B1, drug sensitivity test (H-J), (H) tumor volume change, (I) Gross tumor, and (J) Tumor weight. Abbreviations: G+P, gemcitabine + cisplatin; SUN, sunitinib; EVE, everolimus; TIP, tipifarnib.

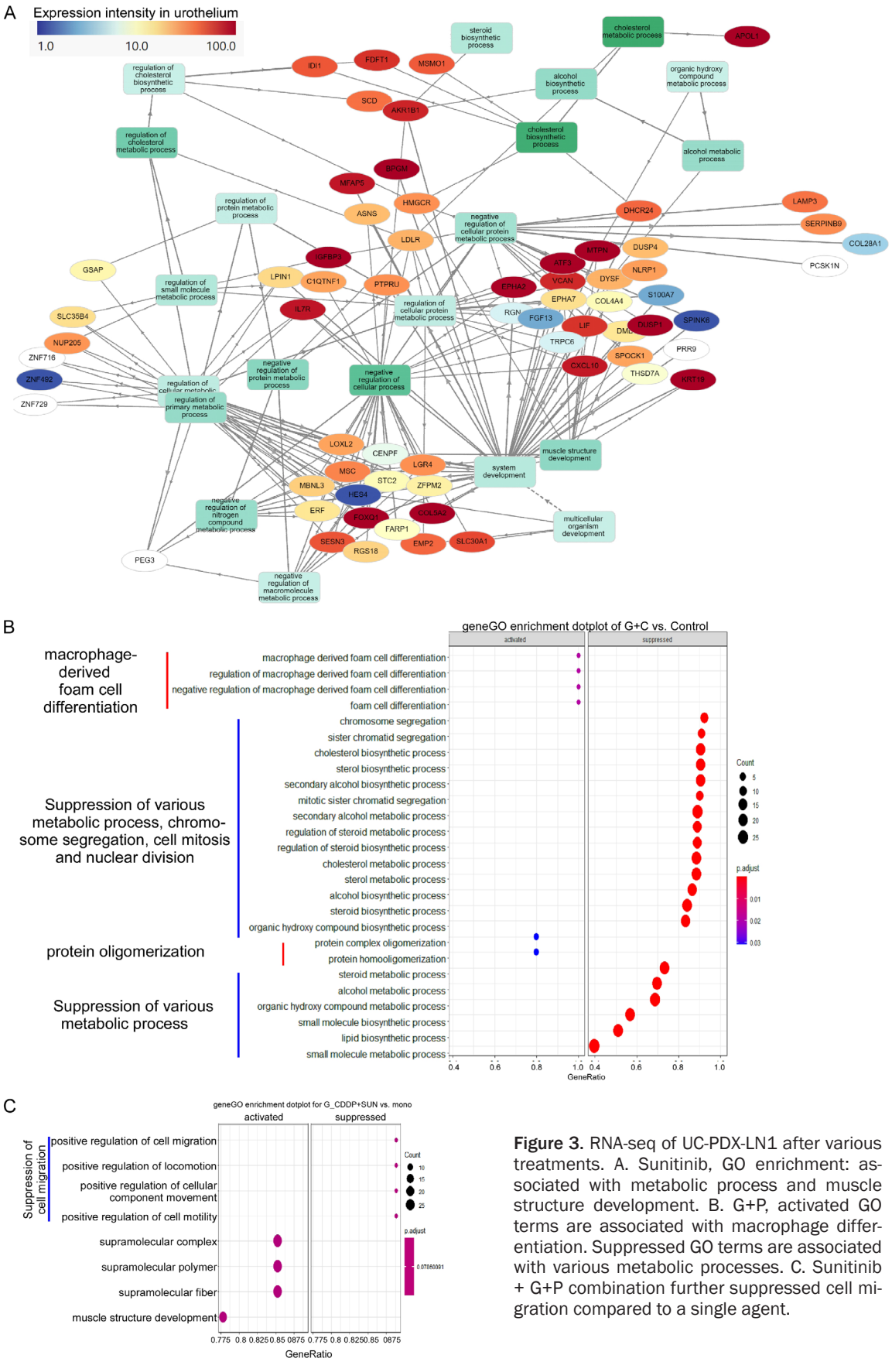

Figure 3. RNA-seq of UC-PDX-LN1 after various treatments. A. Sunitinib, GO enrichment: associated with metabolic process and muscle structure development. B. G+P, activated GO terms are associated with macrophage differentiation. Suppressed GO terms are associated with various metabolic processes. C. Sunitinib + G+P combination further suppressed cell migration compared to a single agent.

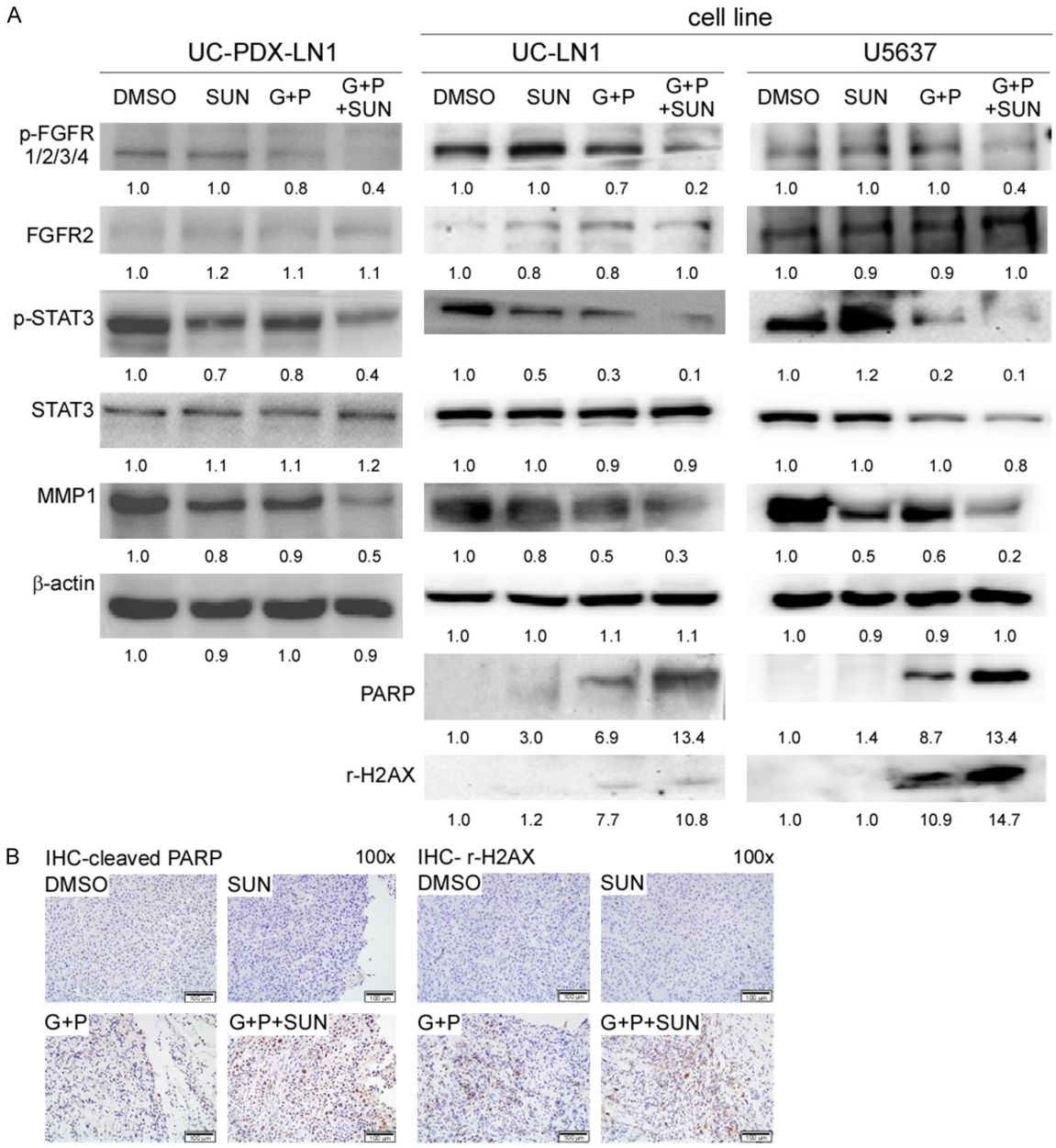

Figure 4. Key protein expression analysis of different pathways after different treatments. A. UC-PDX-LN1 and UC cell lines. UC-LN1 derived from UC-PDX-LN1. B. Immunohistochemistry (IHC) of index protein expression in PDX.

pathways following G+P treatment, which includes the suppression of chromosomal processes. Moreover, the combination of sunitinib and G+P exhibited a synergistic induction of apoptosis and DNA damage, evidenced by a higher level of cleaved PARP and γ-H2AX formation, respectively as shown in right pane of **Figure 4A** and **4B**. Additionally, treatment of UC with sunitinib and G+P effectively suppressed FGFR and STAT3 phosphorylation. The activation of FGFR and STAT3 regulates the expression of downstream proteins associated with cancer formation, progression, and metastasis [26, 27]. This is consistent with functional analysis using differentially expressed genes, indicating that combining sunitinib and G+P inhibited matrix metallopeptidase 1 (MMP1) as illustrated in **Figure 4A**. Therefore, these results suggest that sunitinib and G+P suppress MMP1 through the FGFR and their downstream STAT3

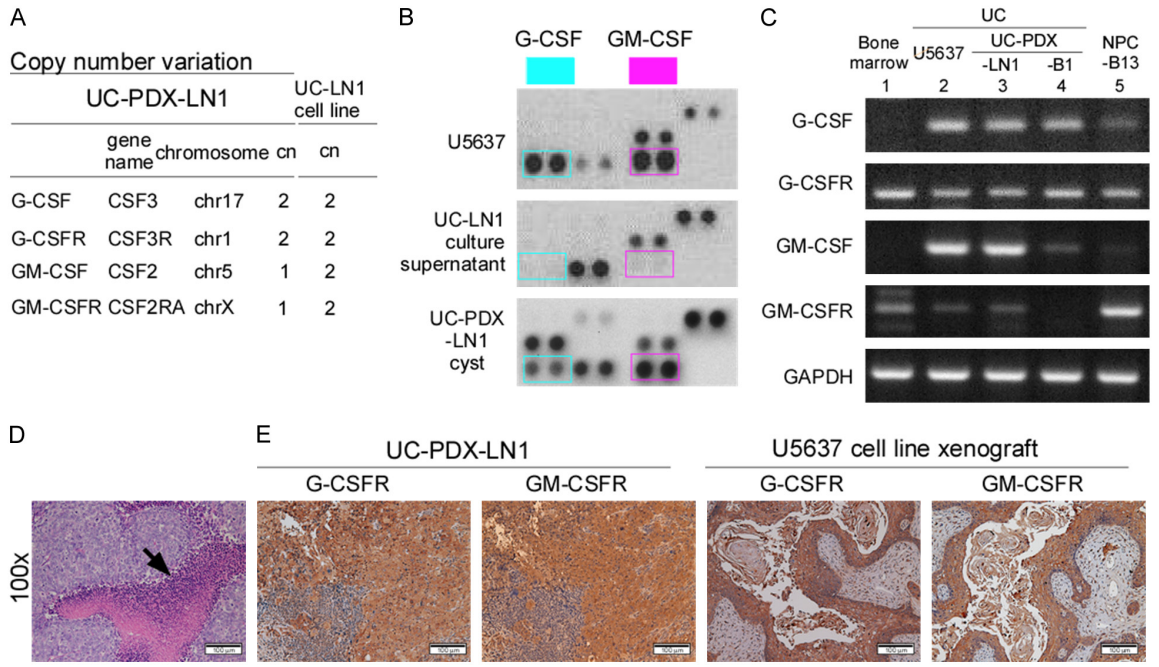

Figure 5. G-/GM-CSF and G-/GM-CSFR in PDX and cell lines. (A) NGS, copy number, (B) G-/GM-CSF cytokine array in different samples and components, (C) mRNA expression in UC PDX, NPC-B13 served as a control. (D) Neutrophil infiltration around the tumor. (E) G-/GM-CSFR expression in UC PDX and cell line xenograft.

signaling pathway, contributing to the suppression of cell migration in UC.

Previous literature has proposed that paraneoplastic leukocytosis may result from the autocrine/paracrine effect of cancer cells secreting granulocyte colony-stimulating factor (G-CSF) and granulocyte-macrophage colony-stimulating factor (GM-CSF) while expressing their respective receptors, G-/GM-CSFR [7, 28]. However, our NGS studies did not reveal mutations or increased copy numbers in G-CSF/GM-CSF and G-CSFR/GM-CSFR genes, as depicted in **Figure 5A**.

In UC-PDX-LN1 tumors, intratumor cystic changes were frequently observed when tumor size exceeded 1000 mm^3. Further investigation using cytokine arrays revealed a rich presence of G-CSF and GM-CSF in the U5637 cell line culture supernatant and UC-PDX-LN1 cyst as demonstrated in **Figure 5B**. RT-PCR confirmed the mRNA expression of myeloid growth pathway genes in our GU PDX lines and cancer cell line, as illustrated in **Figure 5C**. Additionally, in UC-PDX-LN1 tumors, we observed neutrophil infiltration at the border of cysts, as exhibited in **Figure 5D**. Immunohistochemical (IHC) staining further confirmed highly expressed G-CSFR and GM-CSFR in UC-PDX-LN1 and U5637 cell line xenografts, as displayed in **Figure 5E**. These results elucidate that the G-CSF/GM-CSF pathways are actively involved in the tested UC PDX/cell lines.

Paraneoplastic leukocytosis is characterized by the rapid production of a large number of neutrophils in the short term, exhibiting a relatively immature phenotype in peripheral blood. These immature low-density neutrophils (LDNs) can be separated from mature high-density neutrophils (HDNs) after Ficoll-Hypaque density gradient centrifugation [29]. Some LDNs may display a ring-shaped nucleus morphology, indicating a relatively immature stage in neutrophil maturation, as depicted in **Figure 6A**. LDNs exhibit less stringent regulation of NETosis in response to stimulation. Following short-term PMA stimulation, NETosis is more prominent in LDNs compared to HDNs, as demonstrated in **Figure 6B**. RNA-seq analysis comparing LDNs and HDNs from peripheral blood leukocytes of a UC patient revealed upregulated genes in LDNs associated with cellular response to interleukin-8, cell surface receptor signaling pathways, including CXCR1/2, immune response, and neutrophil activation and degranulation (**Figure 6C**).

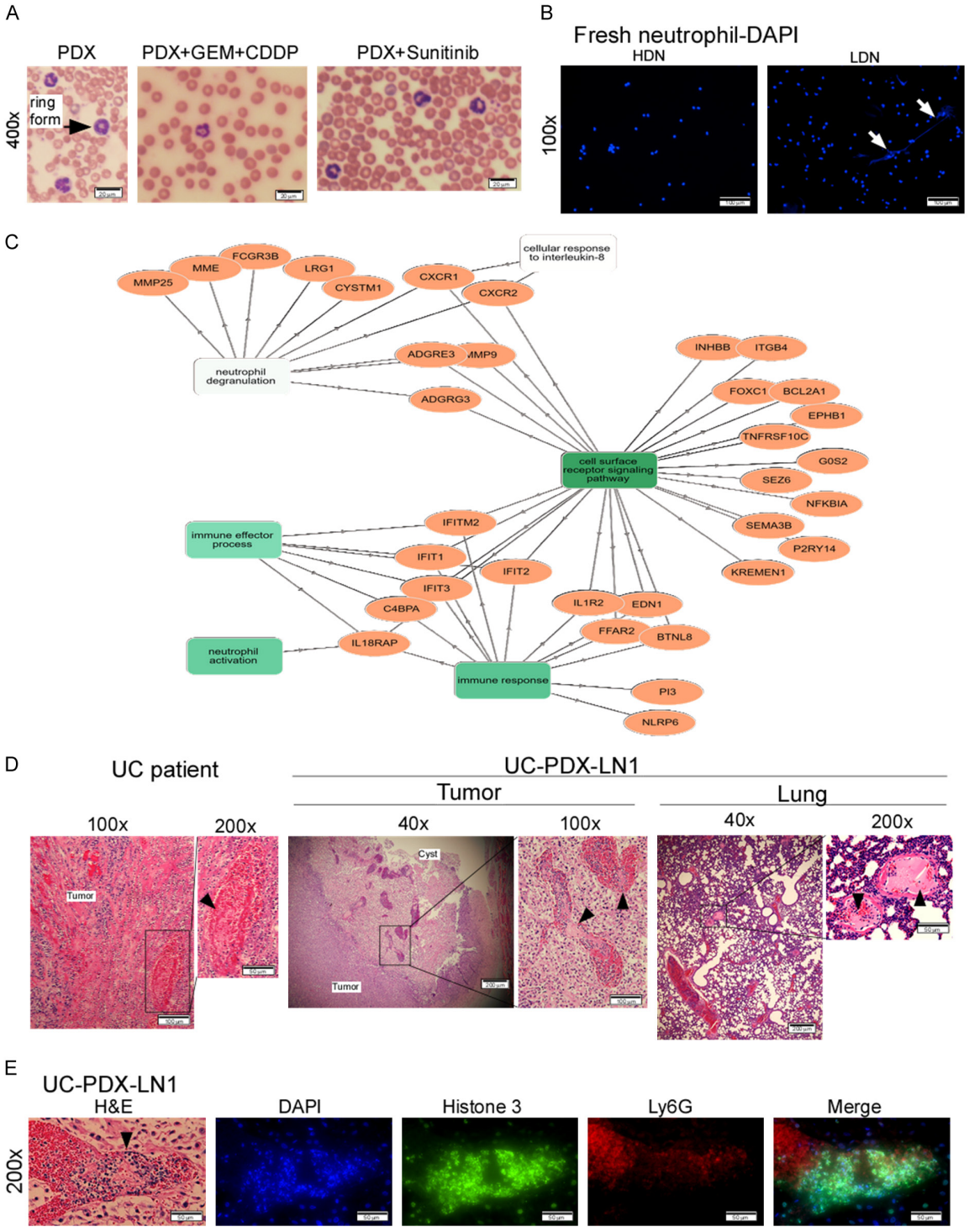

Figure 6. Leukocytosis effect in UC patient and PDX. A. Ring form nucleus of neutrophil existed in peripheral blood (PB) of UC-PDX mice with leukocytosis before but not after treatment. B. Stimulation of NETosis via PMA treatment in low-density neutrophil (LDN) and high-density neutrophil (HDN) from PB of leukocytosis in UC-PDX-LN1. C. RNA-seq comparing between LDN and HDN from PB of leukocytosis UC patient. D. NETosis and related thrombosis in UC patient and PDX in HE staining. Diffuse thromboembolism was found in vessels of the primary patient tumor, PDX tumor, and lung of PDX-implanted mouse (arrowhead: thrombus). E. IHC staining, NETosis with fragmentation of chromosome and histone, and related thrombosis (arrowhead).

NETosis has been shown to induce thrombosis at distant organ sites, such as the lung and kidney, leading to compromised organ failure in a breast cancer model [30, 31]. In our UC patient's tumor and UC-PDX-LN1 implanted mouse, we observed leukocytosis with a neutrophil-dominant presence in small vessels in and around the tumor, extending to distal organs like the lung, and associated with thrombus formation, as shown in **Figure 6D**. IHC staining of UC-PDX-LN1 revealed NETosis with thrombosis around the tumor vessels, as illustrated in **Figure 6E**. These findings provide evidence that tumor-related leukocytosis may induce thrombosis not only systemically but also locally in and around the tumor. The intra/around tumor thromboembolism could retain tumor-secreted cytokines, including G-/GM-CSF, in cysts and further enhance tumor autocrine/paracrine effects, thereby promoting tumor progression.

The interplay between paraneoplastic leukocytosis, NETosis, and thrombosis contributes to enhanced tumor growth and vital organ failure in the current model. To disrupt this vicious cycle, targeting all components - tumor, NETosis, and thromboembolism - emerges as a therapeutic strategy. Ladarixin, a CXCR1/2 inhibitor, while not inhibiting cancer cell line growth in vitro, has shown promise in reducing tumor burden and enhancing immunotherapy in a pancreatic cancer model [32]. In our established UC-LN1 cell line, ladarixin alone demonstrated limited antitumor efficacy with a high IC50 (approximately 40 μM), as depicted in **Figure 7A**. However, in our UC-PDX-LN1 model, ladarixin alone, although showing modest response in gross tumor measurement as illustrated in **Figure 7B**, significantly inhibited tumor growth when evaluated in the solid tumor portion, as illustrated in **Figure 7C**. Additionally, ladarixin treatment reduced neutrophil infiltration and NETosis formation, as shown in **Figure 7E**. Furthermore, the combination of chemotherapy and ladarixin demonstrated enhanced inhibition of PDX growth in solid tumor evaluation, correlating with a reduction in white blood cell count in peripheral blood compared to chemotherapy alone, as depicted in **Figure 7D**.

We also investigated the impact of anti-thrombotic drugs on UC-PDX growth, revealing minimal antitumor response, as depicted in **Figure 8A**. Subsequently, we evaluated the antitumor efficacy of combining chemotherapy with anti-thrombotic medication in our UC-PDX model. While this combination did not surpass chemotherapy alone in terms of antitumor effects (**Figure 8B**), it did extend the survival of PDX-bearing mice, as illustrated in **Figure 8C**. These findings may introduce a novel approach for the clinical management of UC patients with paraneoplastic leukocytosis.

We conducted a retrospective review of bladder cancer (BC) patients at Chang Gung Memorial Hospital, Linkou, Taiwan, from 2010 to 2020. Patient data were analyzed based on the following criteria: (1) histologic diagnosis of urothelial carcinoma of bladder cancer, (2) a white blood cell (WBC) count of > 20,000 cells/mL on two separate occasions with a 30-day interval, and (3) exclusion of identifiable underlying causes for leukocytosis. A total of 2,162 BC patients were assessed, revealing paraneoplastic leukocytosis in 35 patients (1.61%). The median overall survival was 449 days for PNL BC patients, significantly shorter than the 944 days observed for non-PNL BC patients ($P < 0.05$) as shown in **Figure 9**. This outcome suggests a poorer prognosis associated with paraneoplastic leukocytosis in bladder cancer.

Discussion

ERCC2 mutation in GU cancer

ERCC2 encodes the XPD protein, a crucial component of the TFIIH complex involved in general gene transcription and the nucleotide excision repair (NER) pathway [33]. Bladder cancer has been reported to exhibit around 10% mutation in *ERCC2* [34]. Mutations in *ERCC2* often result in a higher mutation load and increased sensitivity to cisplatin-based chemotherapy compared to wild-type *ERCC2*, particularly in muscle-invasive bladder cancer (MIBC) [24, 34]. Most reported *ERCC2* mutations are situated within or around the helicase domain, leading to NER defects, and are associated with a favorable response to cisplatin-based chemotherapy in MIBC [35]. Our UC-PDX model also validates this trend of cisplatin sensitivity.

Target therapy in UC

For recurrent/metastatic head and neck squamous cell carcinoma with a mutant *HRAS* variant allele frequency of ≥ 20%, tipifarnib, a

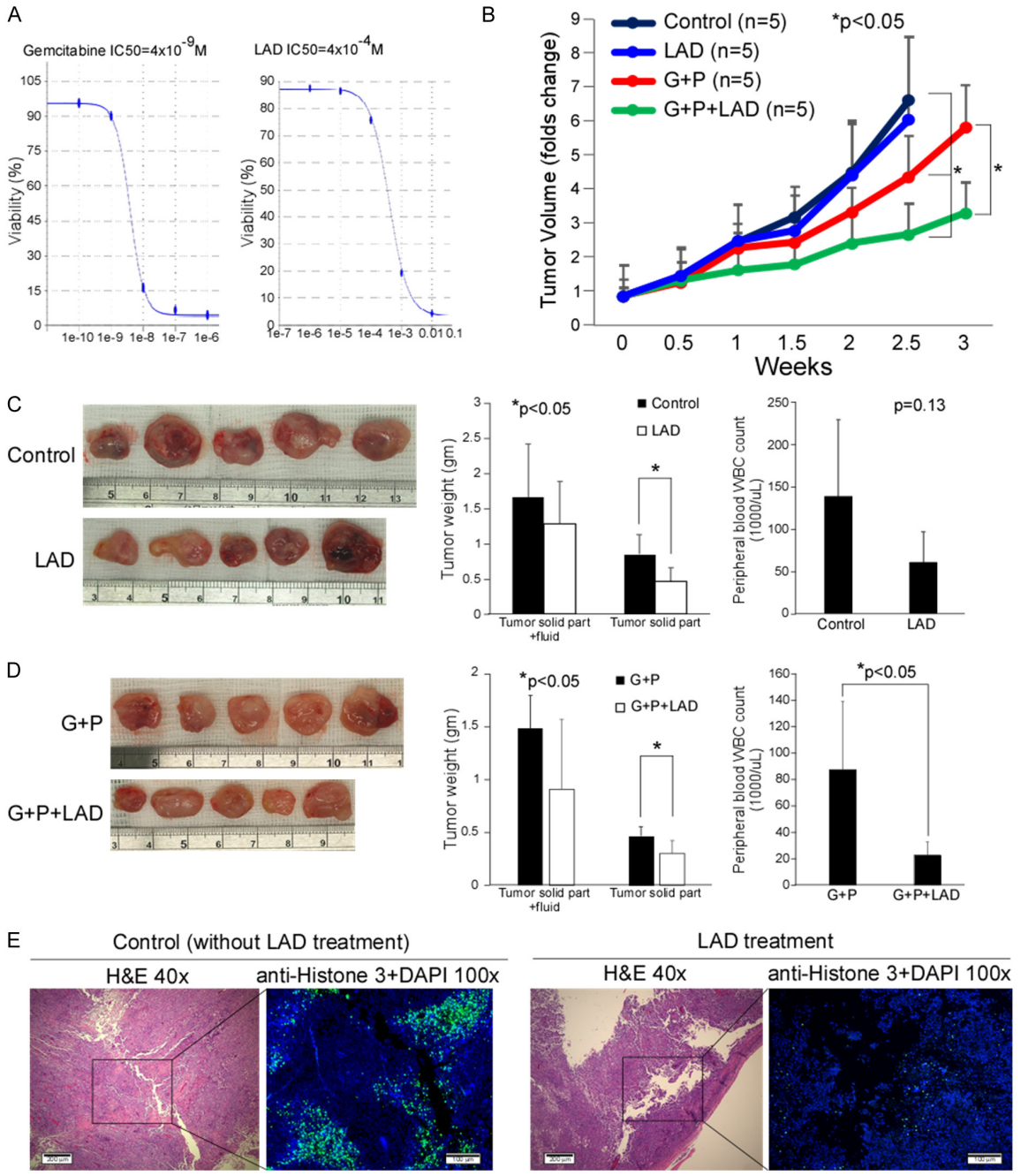

Figure 7. Combination of chemotherapy and anti-neutrophil treatment in GU PDX model. (A) IC50 of gemcitabine and ladarixin, (B-D) Chemotherapy + LAD antitumor effect, tumor volume change in (B), and gross volume, tumor weight, and peripheral blood leukocyte count in (C, D). (E) Ladarixin treatment reduced neutrophil infiltration and NETosis in tumors, without ladarixin (left panel), with ladarixin treatment (right panel). Abbreviations: G+P, gemcitabine + cisplatin; LAD, ladarixin.

farnesyltransferase inhibitor disrupting *HRAS* function, has demonstrated excellent anticancer efficacy [36]. In previously treated/metastatic urothelial carcinoma (UC) harboring *HRAS* mutations, tipifarnib has demonstrated some anticancer efficacy with a manageable safety profile [37]. Despite our UC-PDX-LN1 harboring the Q61R mutation in the *HRAS* gene, tipifarnib did not exhibit any antitumor effect, as illustrated in **Figure 2**.

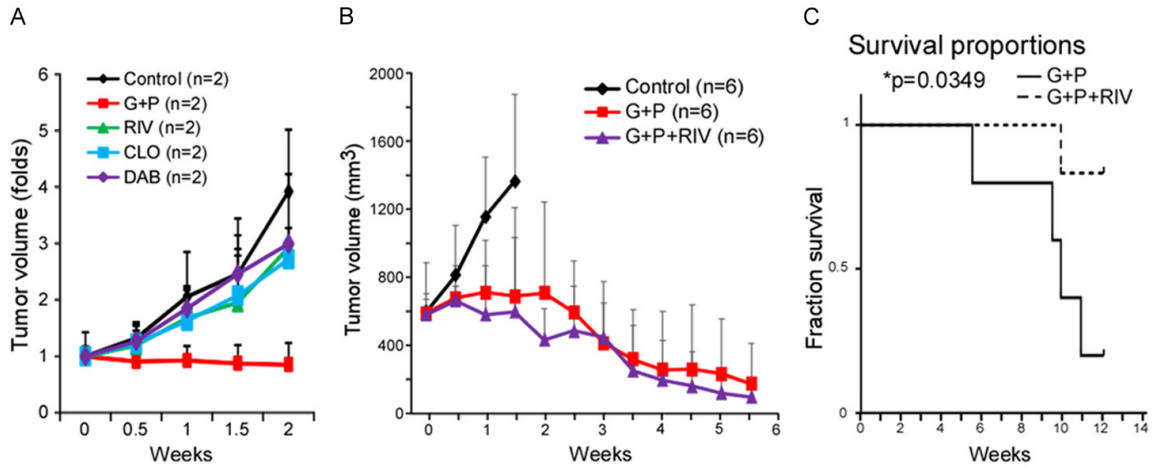

Figure 8. Anticoagulant treatment in GU PDX model. (A) Anticoagulant treatment; (B, C) Combination of chemotherapy and RIV in tumor volume change in (B) and survival of mice in (C). Abbreviations: G+P, gemcitabine + cisplatin; RIV, Rivaroxaban; CLO, Clopidogrel; DAB, Dabigatran.

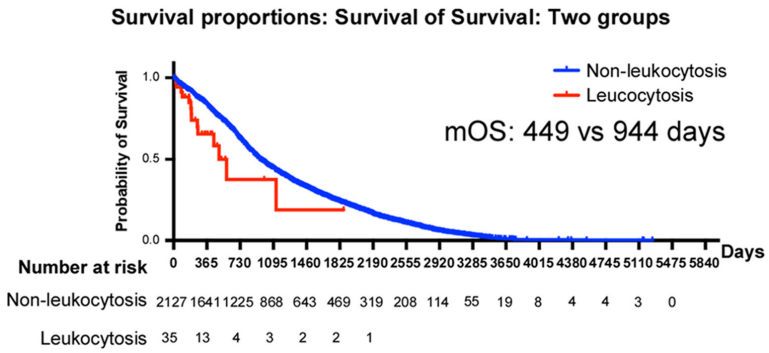

Figure 9. Overall survival of bladder cancer patients, leukocytosis vs. non-leukocytosis. Kaplan-Meier survival analysis showed a median overall survival of 449 days for PNL BC patients compared to 944 days for non-PNL BC patients, with statistical significance ($P < 0.05$).

Sunitinib, a VEGFR inhibitor and potent multiple kinase inhibitor, has demonstrated antitumor efficacy in metastatic UC in clinical trials [38]. Although the combination of gemcitabine and cisplatin (GC) with sunitinib treatment in metastatic UC or muscle-invasive bladder cancer failed in clinical trials due to intolerable side effects, this regimen still exhibited some antitumor efficacy in select patients [39, 40]. In our PDX model drug screening, VEGFR inhibition alone or in combination with chemotherapy may be another option for patients with paraneoplastic leukocytosis. We have also demonstrated that sunitinib can robustly inhibit cisplatin-resistant UC PDX growth, as observed in UC-PDX-B1.

Leukocytosis/NETosis/thromboembolism in UC

Tumors can secrete a broad spectrum of cytokines and chemokines, including G-CSF, TNF-alpha, interleukin-8 (IL-8), and CXCL2, which attract neutrophils, form intratumoral NETosis, and induce an inflammatory tumor microenvironment [41]. IL-8 and its cognate receptors CXCR1/2 can recruit myeloid-derived suppressor cells and neutrophils to the tumor microenvironment, fostering tumor progression [42]. In preclinical models, CXCR1/2 blockers have demonstrated antitumor effects by inhibiting the accumulation of tumor-associated neutrophils in the tumor microenvironment [42, 43]. Ladarixin, a noncompetitive inhibitor of CXCR1/2, has been shown to decrease neutrophil accumulation in a murine model of influenza, improve survival [44], revert tumor-associated M2 macrophage polarization and migration, and enhance immunotherapy in a preclinical pancreatic cancer model [32]. In the current UC PDX model, we found that ladarixin alone sequestered neutrophils infiltrating the tumor, reduced the solid part tumor burden, enhanced chemotherapy's antitumor effect, and ameliorated leukocytosis.

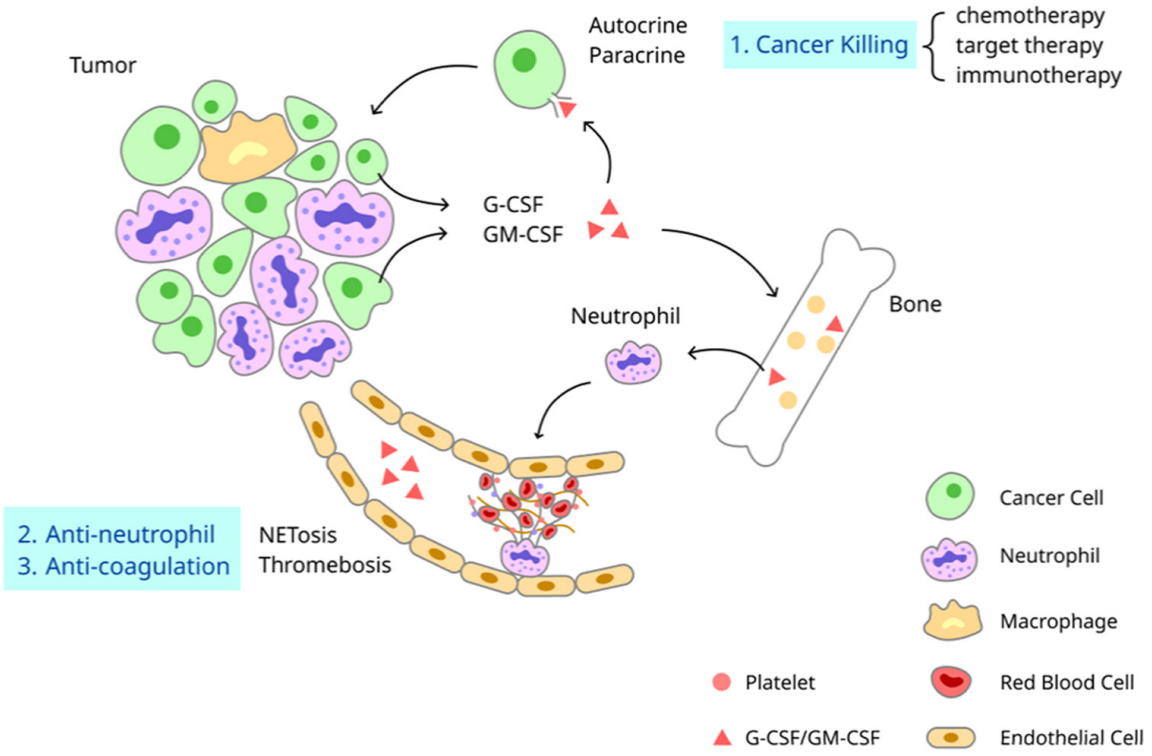

Figure 10. Summary of innovative treatment targets in paraneoplastic leukocytosis/NETosis/thrombosis in UC Patients: 1. Cancer cells secrete growth factors, such as G-CSF and GM-CSF, and express their cognate receptors (G-CSFR or GM-CSFR), initiating autocrine/paracrine loops that enhance tumor growth. 2. Released growth factors stimulate the bone marrow, resulting in the excessive production of neutrophils, contributing to leukocytosis/NETosis/thrombosis. 3. Systemic NETosis/thrombosis may induce vital organ failure at distant sites, while local NETosis/thrombosis can retain growth factors, further amplifying the autocrine/paracrine effect. Utilize a combination of cancer-killing therapies, anti-neutrophil interventions, and anti-coagulation measures to comprehensively disrupt the vicious cycle.

Emerging data indicate that NETosis may induce a hypercoagulable state and increase thromboembolism events in cancer patients, either by NETs themselves or NET degradation products [45]. Low-molecular-weight heparin (LMWH) has been the first-line therapy for venous thromboembolism (VTE) in cancer patients, reducing VTE recurrence [46]. Direct oral anticoagulants (DOACs), such as edoxaban and rivaroxaban, as alternatives to LMWH, have demonstrated non-inferiority for VTE but with a higher incidence of bleeding events [47, 48]. In the present study, we demonstrated that anticoagulants have no direct anticancer effect but may prolong animal survival in combination with chemotherapy compared to chemotherapy alone.

Conclusion

In the present paraneoplastic leukocytosis PDX model as summary in **Figure 10**, we discovered that (1) cancer cells secrete growth factors, such as G-CSF and GM-CSF, and express their cognate receptors (G-CSFR or GM-CSFR), initiating autocrine/paracrine loops that enhance tumor growth; (2) the released growth factors stimulate the bone marrow, resulting in the excessive production of neutrophils, contributing to leukocytosis/NETosis/thrombosis; and (3) systemic NETosis/thrombosis may induce vital organ failure at distant sites, while local NETosis/thrombosis can retain growth factors, further amplifying the autocrine/paracrine effect. Utilizing a combination of cancer-killing therapies, anti-neutrophil interventions, and anti-coagulation measures can comprehensively disrupt the vicious cycle.

Acknowledgements

We thank the staff at the Laboratory Animal Center, Chang Gung Memorial Hospital, Linkou, Taiwan, for animal care and image stud-

ies. This work was supported by grants from the Chang Gung Memorial Hospital, Taiwan (CORPG3J0161~2, C.-L. Hsu) and the Ministry of Science and Technology, Taiwan (MOST-107-2314-B-182-056-MY2, C.-L. Hsu).

Disclosure of conflict of interest

None.

Abbreviations

BC, bladder cancer; CXCR, C-X-C chemokine receptor; G+P, gemcitabine + cisplatin; G-CSF, granulocyte colony-stimulating factor; G-CSFR, granulocyte colony-stimulating factor receptor; GM-CSF, granulocyte-macrophage colony-stimulating factor; GM-CSFR, granulocyte-macrophage colony-stimulating factor receptor; GU, genitourinary; MMP1, matrix metallopeptidase 1; NETs, neutrophil extracellular traps; NGS, next generation sequencing; PNL, paraneoplastic leukocytosis; PDX, patient-derived xenograft; TSP-1, thrombospondin-1; TANs, tumor associated neutrophils; TME, tumor microenvironment; UC, urothelial cell carcinoma.

Address correspondence to: Cheng-Lung Hsu, Division of Hematology-Oncology, Department of Internal Medicine, Chang Gung Memorial Hospital at Linkou, School of Medicine, Chang Gung University, Taoyuan 33305, Taiwan. Tel: +886-3-3281200 Ext. 8825; Fax: +886-3-3278211; E-mail: hsu2221@adm.cgmh.org.tw; Bin Tean Teh, Institute of Molecular and Cell Biology, Agency for Science, Technology and Research (A*STAR), Singapore, The Republic of Singapore. E-mail: teh.bin.tean@singhealth.com.sg

References

[1] Tachibana M, Miyakawa A, Tazaki H, Nakamura K, Kubo A, Hata J, Nishi T and Amano Y. Autocrine growth of transitional cell carcinoma of the bladder induced by granulocyte-colony stimulating factor. Cancer Res 1995; 55: 3438-3443.

[2] Baldwin GC, Gasson JC, Kaufman SE, Quan SG, Williams RE, Avalos BR, Gazdar AF, Golde DW and DiPersio JF. Nonhematopoietic tumor cells express functional GM-CSF receptors. Blood 1989; 73: 1033-1037.

[3] Chakraborty A and Guha S. Granulocyte colony-stimulating factor/granulocyte colony-stimulating factor receptor biological axis promotes survival and growth of bladder cancer cells. Urology 2007; 69: 1210-1215.

[4] Kowanetz M, Wu X, Lee J, Tan M, Hagenbeek T, Qu X, Yu L, Ross J, Korsisaari N, Cao T, Bou-Reslan H, Kallop D, Weimer R, Ludlam MJ, Kaminker JS, Modrusan Z, van Bruggen N, Peale FV, Carano R, Meng YG and Ferrara N. Granulocyte-colony stimulating factor promotes lung metastasis through mobilization of Ly6G+Ly6C+ granulocytes. Proc Natl Acad Sci U S A 2010; 107: 21248-21255.

[5] Singel KL and Segal BH. Neutrophils in the tumor microenvironment: trying to heal the wound that cannot heal. Immunol Rev 2016; 273: 329-343.

[6] Jaillon S, Ponzetta A, Di Mitri D, Santoni A, Bonecchi R and Mantovani A. Neutrophil diversity and plasticity in tumour progression and therapy. Nat Rev Cancer 2020; 20: 485-503.

[7] Granger JM and Kontoyiannis DP. Etiology and outcome of extreme leukocytosis in 758 nonhematologic cancer patients: a retrospective, single-institution study. Cancer 2009; 115: 3919-3923.

[8] Perez FA, Fligner CL and Yu EY. Rapid clinical deterioration and leukemoid reaction after treatment of urothelial carcinoma of the bladder: possible effect of granulocyte colony-stimulating factor. J Clin Oncol 2009; 27: e215-e217.

[9] Izard JP, Gore JL, Mostaghel EA, Wright JL and Yu EY. Persistent, unexplained leukocytosis is a paraneoplastic syndrome associated with a poor prognosis in patients with urothelial carcinoma. Clin Genitourin Cancer 2015; 13: e253-e258.

[10] Hirasawa K, Kitamura T, Oka T and Matsushita H. Bladder tumor producing granulocyte colony-stimulating factor and parathyroid hormone related protein. J Urol 2002; 167: 2130.

[11] Nemeth T, Sperandio M and Mocsai A. Neutrophils as emerging therapeutic targets. Nat Rev Drug Discov 2020; 19: 253-275.

[12] Brinkmann V, Reichard U, Goosmann C, Fauler B, Uhlemann Y, Weiss DS, Weinrauch Y and Zychlinsky A. Neutrophil extracellular traps kill bacteria. Science 2004; 303: 1532-1535.

[13] Albrengues J, Shields MA, Ng D, Park CG, Ambrico A, Poindexter ME, Upadhyay P, Uyeminami DL, Pommier A, Kuttner V, Bruzas E, Maiorino L, Bautista C, Carmona EM, Gimotty PA, Fearon DT, Chang K, Lyons SK, Pinkerton KE, Trotman LC, Goldberg MS, Yeh JT and Egeblad M. Neutrophil extracellular traps produced during inflammation awaken dormant cancer cells in mice. Science 2018; 361: eaao4227.

[14] Sargiannidou I, Qiu C and Tuszynski GP. Mechanisms of thrombospondin-1-mediated metastasis and angiogenesis. Semin Thromb Hemost 2004; 30: 127-136.

[15] Teijeira A, Garasa S, Gato M, Alfaro C, Migueliz I, Cirella A, de Andrea C, Ochoa MC, Otano I, Etxeberria I, Andueza MP, Nieto CP, Resano L, Azpilikueta A, Allegretti M, de Pizzol M, Ponz-Sarvise M, Rouzaut A, Sanmamed MF, Schalper K, Carleton M, Mellado M, Rodriguez-Ruiz ME, Berraondo P, Perez-Gracia JL and Melero I. CXCR1 and CXCR2 chemokine receptor agonists produced by tumors induce neutrophil extracellular traps that interfere with immune cytotoxicity. Immunity 2020; 52: 856-871, e858.

[16] Cools-Lartigue J, Spicer J, McDonald B, Gowing S, Chow S, Giannias B, Bourdeau F, Kubes P and Ferri L. Neutrophil extracellular traps sequester circulating tumor cells and promote metastasis. J Clin Invest 2013; 123: 3446-3458.

[17] Szczerba BM, Castro-Giner F, Vetter M, Krol I, Gkountela S, Landin J, Scheidmann MC, Donato C, Scherrer R, Singer J, Beisel C, Kurzeder C, Heinzelmann-Schwarz V, Rochlitz C, Weber WP, Beerenwinkel N and Aceto N. Neutrophils escort circulating tumour cells to enable cell cycle progression. Nature 2019; 566: 553-557.

[18] Park J, Wysocki RW, Amoozgar Z, Maiorino L, Fein MR, Jorns J, Schott AF, Kinugasa-Katayama Y, Lee Y, Won NH, Nakasone ES, Hearn SA, Kuttner V, Qiu J, Almeida AS, Perurena N, Kessenbrock K, Goldberg MS and Egeblad M. Cancer cells induce metastasis-supporting neutrophil extracellular DNA traps. Sci Transl Med 2016; 8: 361ra138.

[19] Cedervall J, Zhang Y, Huang H, Zhang L, Femel J, Dimberg A and Olsson AK. Neutrophil extracellular traps accumulate in peripheral blood vessels and compromise organ function in tumor-bearing animals. Cancer Res 2015; 75: 2653-2662.

[20] Hsu CL, Lui KW, Chi LM, Kuo YC, Chao YK, Yeh CN, Lee LY, Huang Y, Lin TL, Huang MY, Lai YR, Yeh YM, Fan HC, Lin AC, Lu YJ, Hsieh CH, Chang KP, Tsang NM, Wang HM, Chang AY, Chang YS and Li HP. Integrated genomic analyses in PDX model reveal a cyclin-dependent kinase inhibitor Palbociclib as a novel candidate drug for nasopharyngeal carcinoma. J Exp Clin Cancer Res 2018; 37: 233.

[21] Li HP, Huang CY, Lui KW, Chao YK, Yeh CN, Lee LY, Huang Y, Lin TL, Kuo YC, Huang MY, Fan HC, Lin AC, Hsieh CH, Chang KP, Lin CY, Wang HM, Chao M, Liu JS, Chang YS and Hsu CL. Nasopharyngeal carcinoma patient-derived xenograft mouse models reveal potential drugs targeting cell cycle, mTOR, and autophagy pathways. Transl Oncol 2023; 38: 101785.

[22] Li HP, Huang CY, Lui KW, Chao YK, Yeh CN, Lee LY, Huang Y, Lin TL, Kuo YC, Huang MY, Lai YR, Yeh YM, Fan HC, Lin AC, Hsieh JC, Chang KP, Lin CY, Wang HM, Chang YS and Hsu CL. Combination of epithelial growth factor receptor blockers and CDK4/6 inhibitor for nasopharyngeal carcinoma treatment. Cancers (Basel) 2021; 13: 2954.

[23] Gilardi M, Wang Z, Proietto M, Chilla A, Calleja-Valera JL, Goto Y, Vanoni M, Janes MR, Mikulski Z, Gualberto A, Molinolo AA, Ferrara N, Gutkind JS and Burrows F. Tipifarnib as a precision therapy for HRAS-mutant head and neck squamous cell carcinomas. Mol Cancer Ther 2020; 19: 1784-1796.

[24] Van Allen EM, Mouw KW, Kim P, Iyer G, Wagle N, Al-Ahmadie H, Zhu C, Ostrovnaya I, Kryukov GV, O'Connor KW, Sfakianos J, Garcia-Grossman I, Kim J, Guancial EA, Bambury R, Bahl S, Gupta N, Farlow D, Qu A, Signoretti S, Barletta JA, Reuter V, Boehm J, Lawrence M, Getz G, Kantoff P, Bochner BH, Choueiri TK, Bajorin DF, Solit DB, Gabriel S, D'Andrea A, Garraway LA and Rosenberg JE. Somatic ERCC2 mutations correlate with cisplatin sensitivity in muscle-invasive urothelial carcinoma. Cancer Discov 2014; 4: 1140-1153.

[25] Georgoulis A, Vorgias CE, Chrousos GP and Rogakou EP. Genome instability and gamma-H2AX. Int J Mol Sci 2017; 18: 1979.

[26] Chioni AM and Grose RP. Biological significance and targeting of the FGFR axis in cancer. Cancers (Basel) 2021; 13: 5681.

[27] Wang HQ, Man QW, Huo FY, Gao X, Lin H, Li SR, Wang J, Su FC, Cai L, Shi Y, Liu B and Bu LL. STAT3 pathway in cancers: past, present, and future. MedComm (2020) 2022; 3: e124.

[28] Azuma T, Sakai I, Matsumoto T, Ozawa A, Tanji N, Watanabe A, Uchida N, Narumi H, Yakushijin Y, Hato T, Yasukawa M and Fujita S. Leukemoid reaction in association with bone marrow necrosis due to metastatic prostate cancer. Intern Med 2005; 44: 1093-1096.

[29] Chakraborty S, Keenportz B, Woodward S, Anderson J and Colan D. Paraneoplastic leukemoid reaction in solid tumors. Am J Clin Oncol 2015; 38: 326-330.

[30] Mouchemore KA, Anderson RL and Hamilton JA. Neutrophils, G-CSF and their contribution to breast cancer metastasis. FEBS J 2018; 285: 665-679.

[31] Demers M, Krause DS, Schatzberg D, Martinod K, Voorhees JR, Fuchs TA, Scadden DT and Wagner DD. Cancers predispose neutrophils to release extracellular DNA traps that contribute to cancer-associated thrombosis. Proc Natl Acad Sci U S A 2012; 109: 13076-13081.

[32] Piro G, Carbone C, Agostini A, Esposito A, De Pizzol M, Novelli R, Allegretti M, Aramini A, Caggiano A, Granitto A, De Sanctis F, Ugel S, Corbo V, Martini M, Lawlor RT, Scarpa A and Tortora G. CXCR1/2 dual-inhibitor ladarixin reduces

tumour burden and promotes immunotherapy response in pancreatic cancer. Br J Cancer 2023; 128: 331-341.
[33] Compe E and Egly JM. TFIIH: when transcription met DNA repair. Nat Rev Mol Cell Biol 2012; 13: 343-354.
[34] AACR Project GENIE Consortium. AACR project GENIE: powering precision medicine through an international consortium. Cancer Discov 2017; 7: 818-831.
[35] Li Q, Damish AW, Frazier Z, Liu D, Reznichenko E, Kamburov A, Bell A, Zhao H, Jordan EJ, Gao SP, Ma J, Abbosh PH, Bellmunt J, Plimack ER, Lazaro JB, Solit DB, Bajorin D, Rosenberg JE, D'Andrea AD, Riaz N, Van Allen EM, Iyer G and Mouw KW. ERCC2 helicase domain mutations confer nucleotide excision repair deficiency and drive cisplatin sensitivity in muscle-invasive bladder cancer. Clin Cancer Res 2019; 25: 977-988.
[36] Ho AL, Brana I, Haddad R, Bauman J, Bible K, Oosting S, Wong DJ, Ahn MJ, Boni V, Even C, Fayette J, Flor MJ, Harrington K, Kim SB, Licitra L, Nixon I, Saba NF, Hackenberg S, Specenier P, Worden F, Balsara B, Leoni M, Martell B, Scholz C and Gualberto A. Tipifarnib in head and neck squamous cell carcinoma with HRAS mutations. J Clin Oncol 2021; 39: 1856-1864.
[37] Lee HW, Sa JK, Gualberto A, Scholz C, Sung HH, Jeong BC, Choi HY, Kwon GY and Park SH. A phase II trial of tipifarnib for patients with previously treated, metastatic urothelial carcinoma harboring HRAS mutations. Clin Cancer Res 2020; 26: 5113-5119.
[38] Gallagher DJ, Milowsky MI, Gerst SR, Ishill N, Riches J, Regazzi A, Boyle MG, Trout A, Flaherty AM and Bajorin DF. Phase II study of sunitinib in patients with metastatic urothelial cancer. J Clin Oncol 2010; 28: 1373-1379.
[39] Galsky MD, Hahn NM, Powles T, Hellerstedt BA, Lerner SP, Gardner TA, Yu M, O'Rourke M, Vogelzang NJ, Kocs D, McKenney SA, Melnyk AM Jr, Hutson TE, Rauch M, Wang Y, Asmar L and Sonpavde G. Gemcitabine, Cisplatin, and sunitinib for metastatic urothelial carcinoma and as preoperative therapy for muscle-invasive bladder cancer. Clin Genitourin Cancer 2013; 11: 175-181.
[40] Geldart T, Chester J, Casbard A, Crabb S, Elliott T, Protheroe A, Huddart RA, Mead G, Barber J, Jones RJ, Smith J, Cowles R, Evans J and Griffiths G. SUCCINCT: an open-label, single-arm, non-randomised, phase 2 trial of gemcitabine and cisplatin chemotherapy in combination with sunitinib as first-line treatment for patients with advanced urothelial carcinoma. Eur Urol 2015; 67: 599-602.
[41] Propper DJ and Balkwill FR. Harnessing cytokines and chemokines for cancer therapy. Nat Rev Clin Oncol 2022; 19: 237-253.
[42] Highfill SL, Cui Y, Giles AJ, Smith JP, Zhang H, Morse E, Kaplan RN and Mackall CL. Disruption of CXCR2-mediated MDSC tumor trafficking enhances anti-PD1 efficacy. Sci Transl Med 2014; 6: 237ra67.
[43] Chao T, Furth EE and Vonderheide RH. CXCR2-dependent accumulation of tumor-associated neutrophils regulates T-cell immunity in pancreatic ductal adenocarcinoma. Cancer Immunol Res 2016; 4: 968-982.
[44] Mattos MS, Ferrero MR, Kraemer L, Lopes GAO, Reis DC, Cassali GD, Oliveira FMS, Brandolini L, Allegretti M, Garcia CC, Martins MA, Teixeira MM and Russo RC. CXCR1 and CXCR2 inhibition by ladarixin improves neutrophil-dependent airway inflammation in mice. Front Immunol 2020; 11: 566953.
[45] Rosell A, Martinod K, Mackman N and Thalin C. Neutrophil extracellular traps and cancer-associated thrombosis. Thromb Res 2022; 213 Suppl 1: S35-S41.
[46] Lee AY, Levine MN, Baker RI, Bowden C, Kakkar AK, Prins M, Rickles FR, Julian JA, Haley S, Kovacs MJ and Gent M; Randomized Comparison of Low-Molecular-Weight Heparin versus Oral Anticoagulant Therapy for the Prevention of Recurrent Venous Thromboembolism in Patients with Cancer (CLOT) Investigators. Low-molecular-weight heparin versus a coumarin for the prevention of recurrent venous thromboembolism in patients with cancer. N Engl J Med 2003; 349: 146-153.
[47] Raskob GE, van Es N, Verhamme P, Carrier M, Di Nisio M, Garcia D, Grosso MA, Kakkar AK, Kovacs MJ, Mercuri MF, Meyer G, Segers A, Shi M, Wang TF, Yeo E, Zhang G, Zwicker JI, Weitz JI and Buller HR; Hokusai VTE Cancer Investigators. Edoxaban for the treatment of cancer-associated venous thromboembolism. N Engl J Med 2018; 378: 615-624.
[48] Young AM, Marshall A, Thirlwall J, Chapman O, Lokare A, Hill C, Hale D, Dunn JA, Lyman GH, Hutchinson C, MacCallum P, Kakkar A, Hobbs FDR, Petrou S, Dale J, Poole CJ, Maraveyas A and Levine M. Comparison of an oral factor Xa inhibitor with low molecular weight heparin in patients with cancer with venous thromboembolism: results of a randomized trial (SELECT-D). J Clin Oncol 2018; 36: 2017-2023.

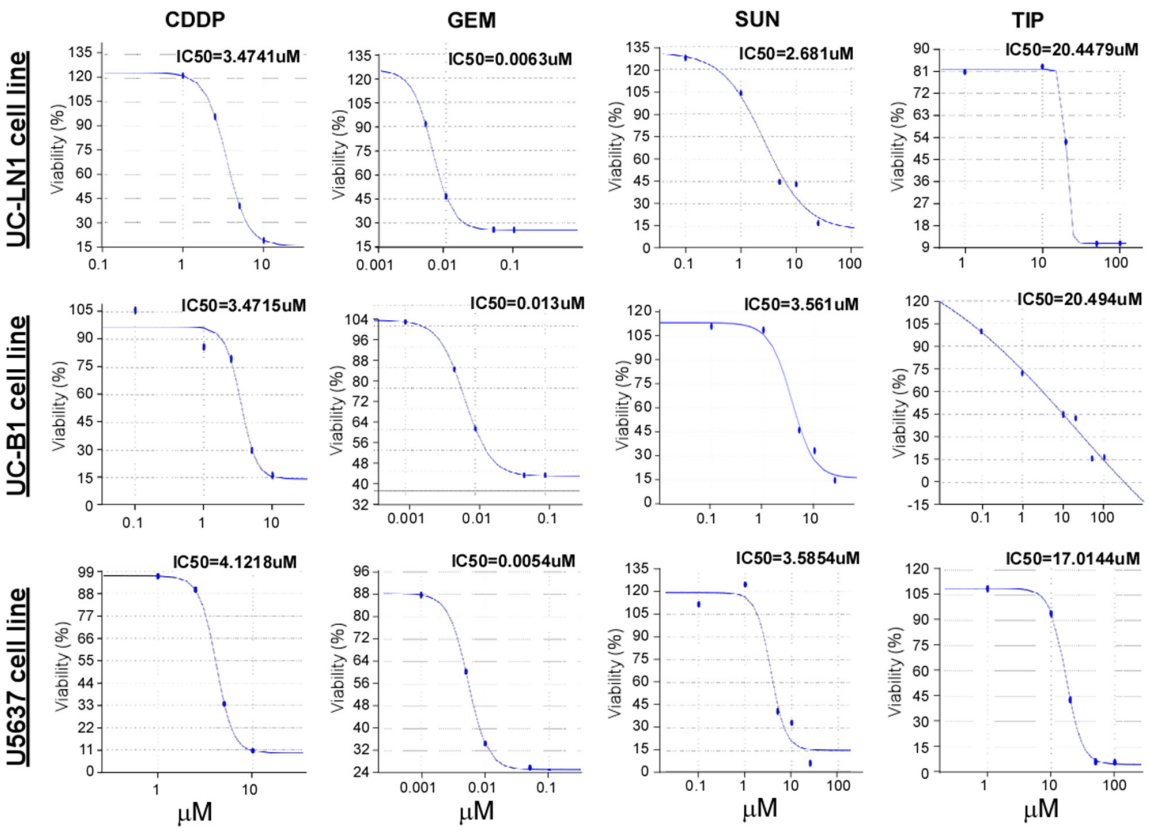

Supplementary Figure 1. The IC50 of cisplatin ranged from 3.4 to 4.1 μM in the tested cell lines, while gemcitabine ranged from 0.0054 to 0.0063 μM in UC-LN1 and U5637. However, it was 0.013 μM in UC-B1, which may reflect a clinical history of treatment resistance (PDX-B1 originated from a clinically gemcitabine-resistant tumor). All the tested cell lines had a low IC50 for sunitinib ranging from 2.6 to 3.5 μM, but were resistant to tipifarnib treatment.